

Key Parameters of High Frequency Welding

Dr. Paul F. Scott
Thermatool Corp
East Haven, CT USA

INTRODUCTION:

In this paper we present a mathematical model for the thermal process that relates the electric current in the weld “vee” to the resulting temperature distribution. The significant conclusion from this study is that the high frequency pipe and tube welding process has two distinct domains of operation, each with its own parameter relationships. The domain in which the process is operating for a given pipe or tube product and mill set-up is determined by mill speed and welding frequency. Operating the production process in the “Thermal Mode”, as opposed to the “Electric Power Mode”, results in the lowest electrical power consumption, the lowest sensitivity to process parameter variation, the lowest impeder magnetic flux level, and the narrowest Heat Affected Zone (HAZ) in the weld area.

MATHEMATICAL MODEL:

The starting point is the physical geometry of the weld “vee” shown in Figure 1. Pipes and tubes generally have walls much thinner than their diameters. For the sake of solvability of the thermal conduction and electrical current density equations, it is reasonable to neglect the curvature of the tube and allow it to extend infinitely in the x direction. This allows the equations to be solved in Cartesian coordinates instead of polar coordinates.

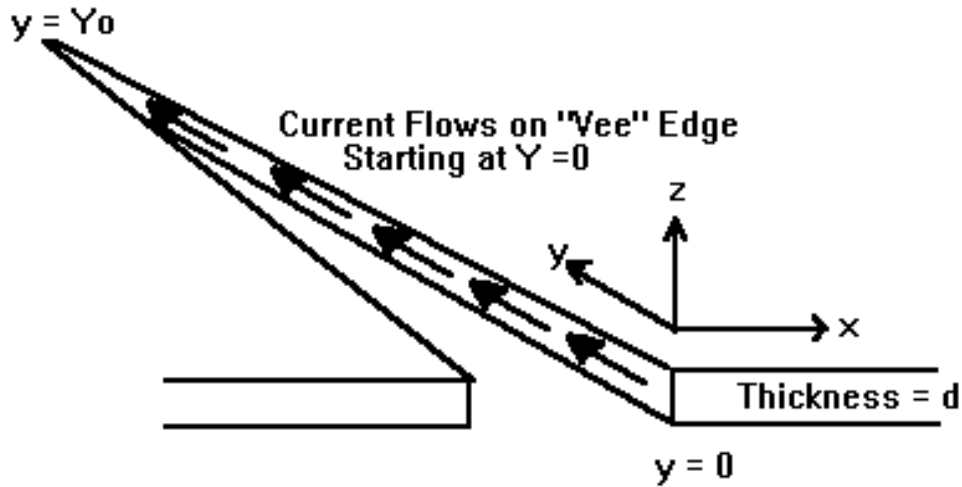


Figure 1 - Weld "Vee" Geometry Used in Thermal Conduction Model

The mathematical model used for studying the “vee” temperature distribution is derived from both the Biot-Fourier equation for thermal conduction:

$$K \nabla^2 T - \rho C_p \frac{dT}{dt} + q = 0 \quad (1)$$

and the equation for current density in an electrically conductive media:

$$\nabla^2 \vec{J} - j2\pi\mu\sigma \vec{J} = 0, \quad (2)$$

a direct result of Maxwell's Equations for electromagnetic phenomena.

The model considers the following effects and variables in describing the pipe or tube welding process:

- Pipe or Tube Dimensions & Mill Set-Up:
 - D is the outside diameter of the pipe or tube,
 - d is the wall thickness of the pipe or tube,
 - v_o is the mill speed,
 - y_o is the length of the weld "vee",
 - and f is the electrical welding frequency.
- Pipe or Tube Material Thermal Properties:
 - T is the temperature distribution in the material,
 - q is the heat generated in the material,
 - K is the thermal conductivity of the pipe or tube material,
 - ρ is the density of the material,
 - and C_p is the heat capacity of the material.
- Pipe or Tube Material Electrical Properties:
 - σ is the electrical conductivity of the pipe or tube material,
 - and μ is its magnetic permeability of the pipe or tube material.

We will assume that the "vee" is heated by a high frequency electric current flowing uniformly along its face and that the penetration into it is limited by "skin effect". "Skin Effect" is a phenomenon directly predictable from the current density equation, Equation 2ⁱ. Simply stated: "At high frequencies, electrical currents and magnetic fields exist only in a thin layer at a conductor's surface". In fact, direct solution of Equation 2 shows that the current density decays exponentially from the surface into a conductor, and the rate of decay is determined by the electrical conductivity, and magnetic permeability of the conductor, and by the frequency of the electric current. The distance it takes for the current density to decay to e^{-1} of its value at the surface is called the "skin depth" or "electrical reference depth" of the conductor. This can be determined from:

$$\xi = \sqrt{\frac{1}{\pi f \mu \sigma}} \quad (3)$$

where ξ is the "skin depth" or "electrical reference depth".

. With a total electric current in the "vee" edge of I_o , starting to flow at $y = 0$, the current density in the tube material is determined by solving Equation 2:

$$\vec{J} = \frac{I_o}{d\xi} e^{-x/\xi} \vec{i}_y \quad (4)$$

Heat is generated at the "vee" edge by electrical resistive power loss. The power density in the pipe or tube causing this heating is:

$$q_o = \frac{|\vec{J}|^2}{\sigma} = \frac{I_o^2 e^{-2x/\xi}}{d^2 \xi^2 \sigma} \quad (5)$$

It is important to note that the effective “skin depth” or e^{-1} depth for the power density is half of that for the electric current or magnetic field. We will define the “electric power reference depth” as $\xi/2$.

We turn now to the solution of the Biot-Fourier Equation. The spatial variables and derivatives in Equation 1 are in a coordinate system relative to an element of pipe or tube material (“Lagrangian Coordinates”). Recognizing that in a coordinate system relative to the mill (“Eulerian Coordinates”), we have a “steady state” temperature distribution and that heat is transferred by material convection (heat moves with the tube material at the mill speed), we transform Equation 1 by replacing the time derivative with:

$$\frac{dT}{dt} = \frac{dT}{dy} \frac{dy}{dt} = v_o \frac{dT}{dy} \quad (6)$$

where y is now the distance along the “vee” in mill coordinates, and v_o is the mill speed. With the further assumption that thermal conduction in the pipe or tube strip is essentially away from the “vee” in the x direction, we rewrite the thermal conduction equation as:

$$K \frac{d^2 T(x, y)}{dx^2} - \rho C_p v_o \frac{dT(x, y)}{dy} + Q_o e^{-2x/\xi} \mu_{-1}(y) = 0 \quad (7)$$

where $\mu_{-1}(y)$ is the unit step function and is used to signify that the electric current starts flowing along the tube edge at $y = 0$, and:

$$Q_o = \frac{I_o^2}{d^2 \xi^2 \sigma} \quad (8)$$

is the power density at the edge of the “vee”.

The differential equation can be solved for the temperature distribution along the edge of the “vee”, defining the “vee” length as y_o . This procedure is fairly tedious so it is outlined in Appendix I.

Boundary conditions are applied that assume the starting or ambient temperature is zero:

$$T(x, y = 0) = T(x \rightarrow \infty, y) = 0 \quad (9)$$

so that the resulting temperature distribution represents the temperature rise at the edge, not the absolute temperature. Further, it is assumed that no heat is lost at the edge of the “vee” so that :

$$\left. \frac{dT(x, y)}{dx} \right|_{x=0} = 0 \quad (10)$$

and finally, the forge temperature rise at the end of the “vee” is defined to be ΔT :

$$T(x = 0, y = y_o) = \Delta T \quad (11)$$

The resulting solution for the “vee” edge temperature is now rearranged to get an equation for the power applied to the “vee” as a function of the critical process parameters. This total applied power is:

$$P_o = 2y_o d Q_o \int_0^\infty e^{-2x/\xi} dx = d y_o \xi Q_o \quad (12)$$

where the factor of “two” results from the fact that both sides of the “vee” must be heated. The final result for total “vee” power as a function of the critical process parameters is:

$$P_o = \frac{3\sqrt{\pi}\Delta T y_o d K}{\xi \sqrt{\alpha} \left[\left(\frac{4y_o \varepsilon}{\xi^2 v_o \alpha} + 1 \right)^{3/2} - \left(\frac{4y_o \varepsilon}{\xi^2 v_o \alpha} \right)^{3/2} - 1 \right]} \quad (13)$$

where:

$$\varepsilon = K / C_p \rho \quad (14)$$

is the thermal diffusivity of the tube material and α is a constant of integral approximation:

$$4/\pi \leq \alpha < 2 \quad (15)$$

Later it will become obvious that α is much closer to $4/\pi$ than to 2.

Equation 13 is the most significant result disclosed in this paper and contains much information about how the high frequency pipe and tube welding process behaves. The first important result comes from the examination of the bracketed term in the denominator. This term has two limiting values depending on whether:

$$\left(\frac{4y_o \varepsilon}{\xi^2 v_o \alpha} \right) < ? > 1 \quad (16)$$

Recognizing that $\left(\frac{y_o}{v_o} \right)$ is the time an element of the “vee” material experiences heating, and that the thermal diffusivity of a material tells us how far heat penetrates in a given amount of time, we can rewrite Equation 16 (setting $\alpha = 4 / \pi$) as:

$$\sqrt{\left(\frac{\pi}{4}\right)\left(\frac{y_o}{v_o}\right)}\varepsilon < ? > \left(\frac{\xi}{2}\right) \quad (17)$$

The left side can be recognized as the distance into the “vee” edge heat will diffuse by thermal conduction, and is the classical definition of “thermal reference depth” in a material. The right side of the equation is the depth of heating due to the electric current on the “vee” edge, the “electric power reference depth”.

If the “electric power reference depth” is larger than the “thermal reference depth”, the characteristics of the welding process will be controlled by electrical “skin effect”. We will call this the “Electric Power Mode” of the process. If the “thermal reference depth” is larger than the “electrical power reference depth”, the characteristics of the welding process will be controlled by thermal conduction. We will call this the “Thermal Mode” of the process.

Thus there are two distinct modes of operation for the process and the effects of the critical process parameters can be expected to be different depending on which mode the process is operating in. Another way to view the separation between the operational modes for the welding process is to recast equation 16 as an equality. This result contains material properties, the mill speed, the welding frequency, and the “vee” length. It is a recommended practice in pipe and tube welding to set the “vee” length roughly equal to the pipe or tube outside diameter. If we do this, we can obtain a set of curves for “Critical Mill Speed” as a function of welding frequency and pipe or tube outside diameter for a particular pipe or tube material. If the welding process is operated with a mill speed reasonably above the “Critical Mill Speed”, the welding process will be in the “Electric Power Mode”. If the welding process is operated reasonably below the “Critical Mill Speed”, the welding process will be in the “Thermal Mode”. The equation for the “Critical Mill Speed” is:

$$v_{critical} = \pi^2 \mu \sigma \varepsilon f y_o = \pi^2 \mu \sigma \varepsilon f D \quad (18)$$

where D is the pipe or tube outside diameter. The value of the “Critical Mill Speed” is graphed for mild steel as a function of pipe or tube diameter and for several welding frequencies in Figure 2.

Equation 17 may also be used to define a “Critical Welding Frequency”. Like the “Critical Mill Speed”, the “Critical Welding Frequency” determines the boundary between the two process modes. When the process is operated reasonably below the “Critical Welding Frequency”, the process is in the “Electric Power Mode”, and when it is operated reasonably above the “Critical Welding Frequency” it is in the “Thermal Mode”. The “Critical Welding Frequency” is defined as:

$$f_{critical} = \frac{v_o}{\pi^2 \varepsilon y_o \mu \sigma} \quad (19)$$

If the “vee” length is equal to the pipe or tube diameter, we may plot the “Critical Welding Frequency” as a function of mill speed for several different tube diameters. This is done in Figure 3.

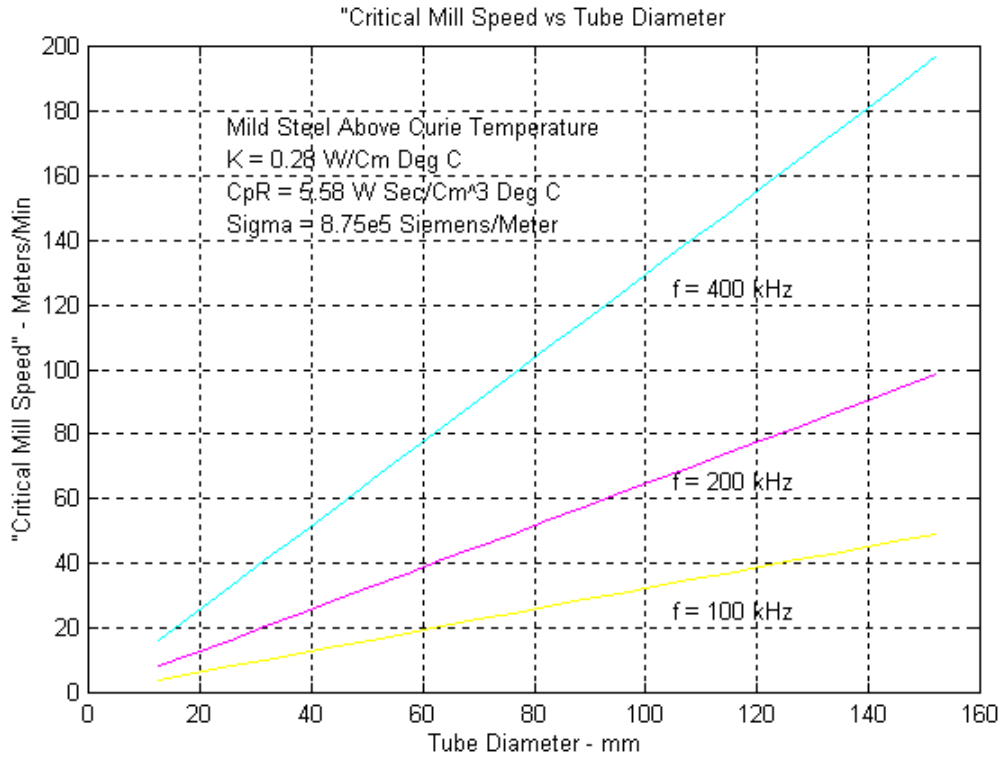


Figure 2 - "Critical Mill Speed" as a Function of Tube Diameter

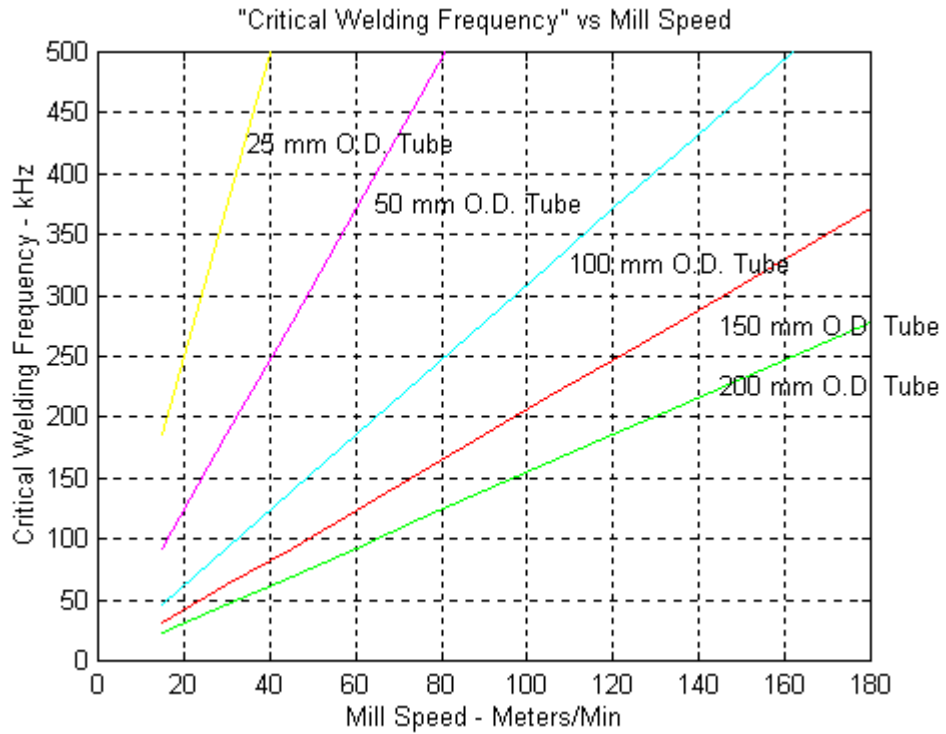


Figure 3 - "Critical Welding Frequency" as a Function of Mill Speed

Results can also be obtained for the “vee” power requirement reasonably above, at, and reasonably below the “Critical Welding Frequency”. The term in the brackets in the denominator of Equation 13 can be expanded in an appropriate binomial series and higher order terms discarded. This is carried out in Appendix II. Also, it is reasonable to assume that the Heat Affected Zone (HAZ) in the pipe or tube edge will be roughly equal to twice the “reference depth” that controls the heating. The factor of two allows for a measurement across both sides of the “vee”. These results are:

“Thermal Mode” or $f_{Operating} \gg f_{Critical}$:

$$P_o \cong \Delta T d \sqrt{\pi y_o K C_p \rho v_o} \quad (20)$$

$$HAZ \cong 2 \sqrt{\left(\frac{\pi}{4}\right) \left(\frac{y_o}{v_o}\right) \epsilon} = \sqrt{\pi \left(\frac{y_o}{v_o}\right) \epsilon} \quad (21)$$

“Transition Region” or $f_{Operating} = f_{Critical}$:

$$P_o = \left[\frac{3}{4(\sqrt{2} - 1)} \right] \Delta T d \sqrt{\pi y_o K C_p \rho v_o} = 1.81 \Delta T d \sqrt{\pi y_o K C_p \rho v_o} \quad (22)$$

and for:

“Electric Power Mode” or $f_{Operating} \ll f_{Critical}$:

$$P_o \cong 2 \Delta T C_p \rho d \left(\frac{\xi}{2}\right) v_o = \frac{\Delta T C_p \rho d v_o}{\sqrt{\pi f \mu \sigma}} \quad (23)$$

$$HAZ \cong 2 \left(\frac{\xi}{2}\right) = \frac{1}{\sqrt{\pi f \mu \sigma}} \quad (24)$$

The results above show us that when the welding frequency is below the “Critical Welding Frequency”, increasing the welding frequency will reduce the weld power requirement (improving the process efficiency) and also reduce the width of the Heat Affected Zone. When operating well above the “Critical Welding Frequency”, both the power requirement and heat affected zone are insensitive to frequency. It is important to note that no penalty is incurred for welding above the “Critical Welding Frequency”. Examination of Equations 20 and 22 tells us that welding at the “Critical Welding Frequency” requires 80% more power in the “vee” than welding well above it. Welding below the “Critical Welding Frequency” results in a still higher power requirement and a wider Heat Affected Zone. Also note that the discussion to this point has only dealt with thermal considerations. Minimally, the welding frequency should be chosen so that the “electrical reference depth” in the pipe or tube material below the Curie temperature is at least one fifth of the wall thickness. This ensures good inductive coupling between the work coil and the pipe or tube.

Also affected by which mode the process is operating in is the sensitivity of the weld power requirement due to variations in the process parameters. If the process is operating in the “Electric

Power Mode”, weld power varies proportionally to the thermal constants characterizing the pipe or tube material, and the mill speed. However, in the “Thermal Mode”, the weld power varies as the square root of these quantities. Additionally, in the “Electric Power Mode”, the weld power depends on the welding frequency, and the electrical constants of the pipe or tube material. In the “Thermal Mode”, the welding power is independent of these quantities. Thus, it is easy to see that if the process is operated in the “Thermal Mode”, as opposed the “Electric Power Mode”, it will be far less sensitive to process parameter variations.

Finally, it is possible to calculate the magnetic flux required in the impeder necessary to transfer the power required to achieve the forge welding temperature. Equations 8 and 12 are used to rewrite Equation 13 to express the “vee” current required to achieve the forge temperature. This can be used to calculate the magnetic flux in the “vee”. Gauss’ Law is then used to calculate the impeder flux. The result is that:

$$|B_{Im\ peder}| = \left[\frac{A_{\text{“vee”}}}{A_{Im\ peder}} \right] \mu_o \sqrt{\frac{3\pi K \Delta T \sigma}{2 \left[\left(\frac{f}{f_{Critical}} + 1 \right)^{3/2} - \left(\frac{f}{f_{Critical}} \right)^{3/2} - 1 \right]}} \quad (25)$$

where: $|B_{Im\ peder}|$ is the magnitude of the magnetic flux in the impeder,
 $A_{\text{“vee”}}$ is the area of the weld “vee”,
 $A_{Im\ peder}$ is the cross-sectional area of the impeder,
and μ_o is the magnetic permeability of free space.

Analysis of this equation shows that when the process is in the “Electric Power Mode”, the impeder flux is approximately:

$$|B_{Im\ peder}| \cong \left[\frac{A_{\text{“vee”}}}{A_{Im\ peder}} \right] \mu_o \sqrt{\frac{\Delta T C_p \rho v_o}{\pi \mu y_o f}} \quad (26)$$

and when the process is operating in the Thermal Mode, the impeder flux is approximately:

$$|B_{Im\ peder}| \cong \left[\frac{A_{\text{“vee”}}}{A_{Im\ peder}} \right] \mu_o (\Delta T)^{1/2} \left[\frac{K C_p \rho \sigma v_o}{\mu y_o f} \right]^{1/4} \quad (27)$$

These equations show that the impeder flux is reduced as $f^{-1/2}$ as welding frequency increases until the process transitions from the “Electric Power Mode” to the “Thermal Mode”. Then the impeder flux continues to decrease but at the slower rate of $f^{-1/4}$. A representative plot of impeder magnetic flux level as a function of welding frequency for small diameter tubing is shown in Figure 4.

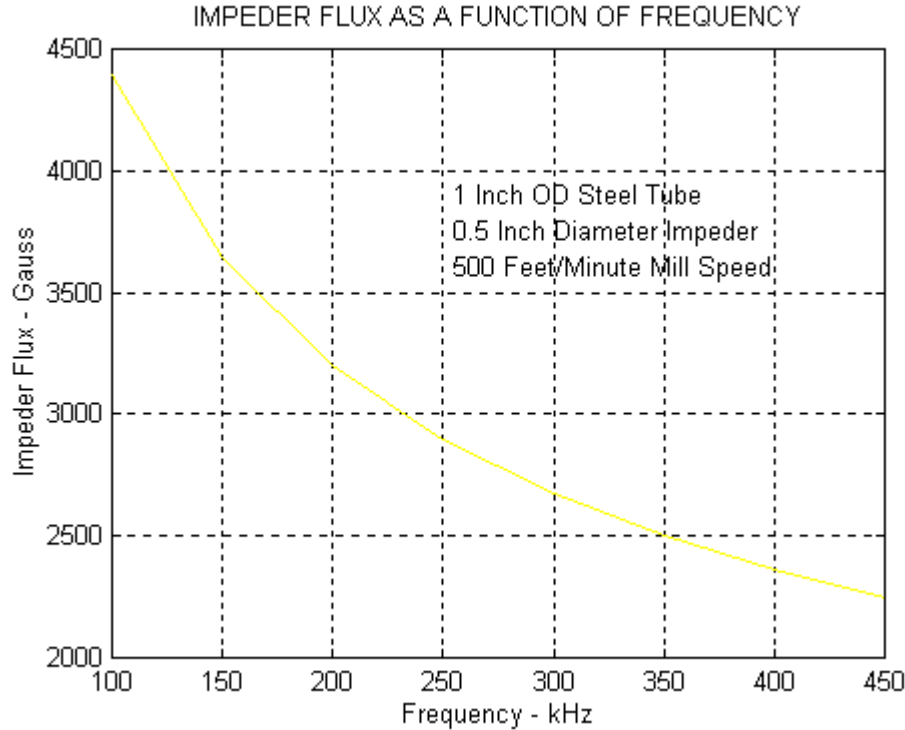


Figure 4 - Impeder Magnetic Flux vs Welding Frequency for Small Tubing

So far we have shown that the induction welding process used in pipe and tube fabrication has two modes of operation, the “Thermal Mode” and the “Electric Power Mode”. Given a choice, which is the best mode for pipe and tube fabrication? It should be clear from the preceding analysis that the “Thermal Mode” provides several advantages over the “Electric Power Mode”. Specifically, operating the process in the “Thermal Mode” results in:

- The lowest welding power requirement, hence the highest efficiency.
- The narrowest Heat Affected Zone, hence the best weld quality.
- The least sensitivity to variations in process parameters.
- The lowest impeder magnetic flux level, providing the maximum margin against impeder flux saturation.

Operation of the process in the “Thermal Mode” is best accomplished by selecting a welding frequency sufficiently above the “Critical Welding Frequency” as defined in Equation 19 for the fastest anticipated mill speed for the pipe or tube materials and sizes to be manufactured.

EXPERIMENTAL VALIDATION OF THE MATHEMATICAL MODEL:

To validate the mathematical model presented above, the same tube was produced at three mill speeds and several different welding frequencies ranging from 100 kHz to 400 kHz. The mill set-up and “vee” temperature, as measured with a two color optical pyrometer, were held constant and the power required to achieve this temperature was recorded. Samples were taken from each lot of tubing

and the Heat Affected Zone was measured using standard metallurgical techniques. This data was compared with predictions from the mathematical model using Equation 13 and Equations 21 and 24.

Specifically, the tube and its production process had the following characteristics:

Strip Material	Low Carbon Steel
Strip Width	120.2 mm
Strip Thickness	1.47 mm
Tube O. D. - Before Weld Rolls	39 mm
Tube O. D. - After Weld Rolls	38.75 mm
Squeeze Out	0.8 mm
“Vee” Length	38.1 mm
Impeder Material	TDK IP-1
Impeder Diameter	19.4 mm
Impeder Length	330 mm
Impeder Location	Leading Edge 241 mm from End of “Vee”
Welding Temperature (ΔT)	1400 Degrees C
Assumed Thermal Conductivity (K)	0.28 Watts/Cm Degrees C
Assumed Heat Capacity Times Density ($C_p\rho$)	5.58 Watt Seconds/Cm ³ Degrees C
Assumed Electrical Conductivity (σ)	8.75 x 10 ⁵ Siemens/Meter

The data collected for weld power requirement and calculated values from Equations 13 and 19 are recorded below in Table 1.

TABLE 1 - Experimental Data for Welding Power Requirement

Mill Speed (Meters/Min)	Welding Frequency (kHz)	Welder Output Power (kW)	$f_{welding} / f_{critical}$	“Vee” Power from Eq. 12 (kW)	$\frac{\text{“Vee” Power}}{\text{Welder Output Power}}$ (Per Cent)
30.5	130	40	0.53	12.10	30.3
30.5	226	36	0.91	10.40	28.9
30.5	270	34	1.09	10.00	29.3
30.5	352	33	1.42	9.36	28.4
30.5	401	34	1.62	9.09	26.8
61	130	76	0.26	21.5	28.3
61	216	64	0.44	18.2	28.4
61	270	61	0.55	17.0	27.8
61	350	55	0.71	15.8	28.7
61	400	53	0.81	15.2	28.7
91.5	216	94	0.29	25.4	27.0
91.5	260	92	0.35	23.9	26.0
91.5	280	88	0.38	23.3	26.5
91.5	320	84	0.43	22.3	26.6
91.5	420	82	0.57	20.6	25.1

These results show a reasonably constant efficiency between the power output of the welder and the “vee” power calculated from Equation 13, despite a variation in $f_{welding} / f_{critical}$ from 0.26 to 1.62. The slight fall-off in efficiency as both frequency and power are increased is attributed to

“I²R” losses in the work coil and buss work. The over-all efficiency can be estimated using “least squared error” techniques to be 28.9% and agrees very well with other determinations of the efficiency of the high frequency welding processⁱⁱ. Using this value to fit the welder output power to the calculated “vee” power for all three speeds, we obtain the graph shown as Figure 5. It is clear that the mathematical model predicts the experimental data very well.

The heat affected zone (HAZ) was also measured for each sample of tube produced. This data is shown below in Table 2. Figures 6, 7, and 8 are graphs of this data, one for each of the three mill speeds. Also shown on these plots are the electrical and thermal limits for the Heat Affected Zone predicted by Equations 21 and 24. Figure 8, where tube was produced at 91.5 meters per minute, illustrates the case where the welding frequency is much below the “Critical Welding Frequency”. We expect from our mathematical model that the Heat Affected Zone will be roughly twice the electric power reference depth and the figure shows that the measured heat affected zone tracks the evaluation of Equation 24 very well. In Figure 7, data taken for tube made at 60.5 meters per minute, the welding frequency starts to approach the “Critical Welding Frequency”. As expected from the mathematical model, the Heat Affected Zone is now determined by both the thermal and electric power reference depths, and is now larger than either of them. Finally, Figure 6 showing data taken at 30.5 meters per minute, illustrates the case where the welding frequency transitions above the critical frequency. At the critical weld frequency, it can be seen that the heat affected zone is about 40% larger than either twice the thermal or electric power reference depth. Finding an exact, mathematical solution for Heat Affected Zone in this transition region is a subject of our on-going research.

TABLE 2 - Experimental Data for Heat Affected Zone (HAZ)

Mill Speed (Meters/Min)	Welding Frequency (kHz)	Measured HAZ (mm)	$\frac{f_{welding}}{f_{critical}}$	Thermal Limit (Equation 19) (mm)	Electrical Limit (Equation 22) (mm)
30.5	130	2.03	0.53	1.08	1.49
30.5	226	1.55	0.91	1.08	1.13
30.5	270	1.52	1.09	1.08	1.03
30.5	352	1.55	1.42	1.08	0.91
30.5	401	1.37	1.62	1.08	0.85
61	130	1.37	0.26	0.76	1.49
61	216	1.17	0.44	0.76	1.16
61	270	1.19	0.55	0.76	1.03
61	350	1.04	0.71	0.76	0.91
61	400	1.04	0.81	0.76	0.85
91.5	216	1.02	0.29	0.62	1.16
91.5	260	1.02	0.35	0.62	1.05
91.5	280	0.99	0.38	0.62	1.02
91.5	320	0.97	0.43	0.62	0.95
91.5	420	0.89	0.57	0.62	0.83

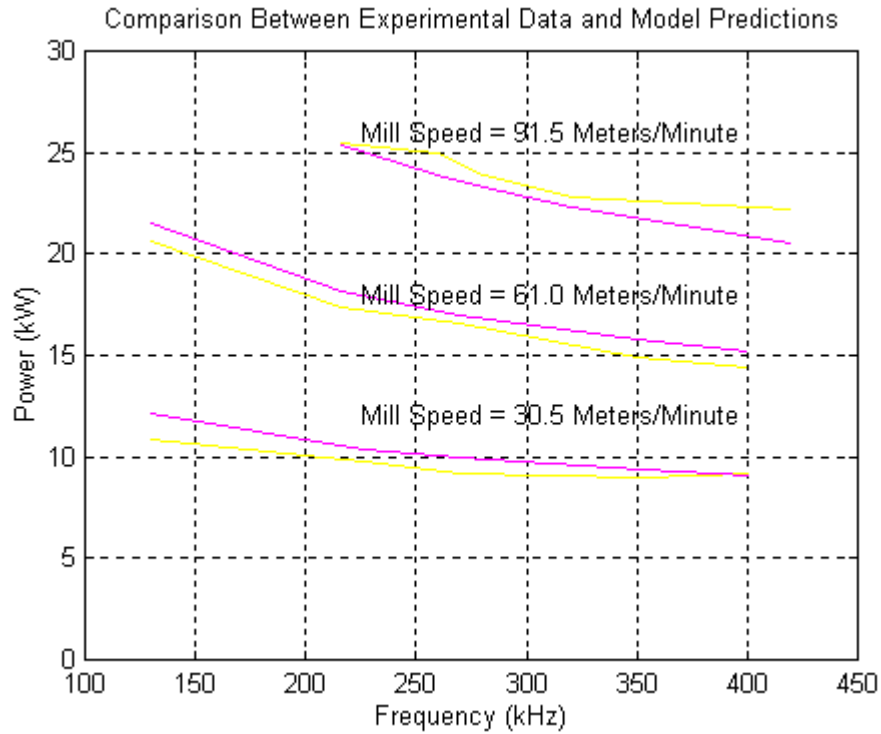


Figure 5 - Comparison of Experimental and Calculated Power in Weld “Vee”

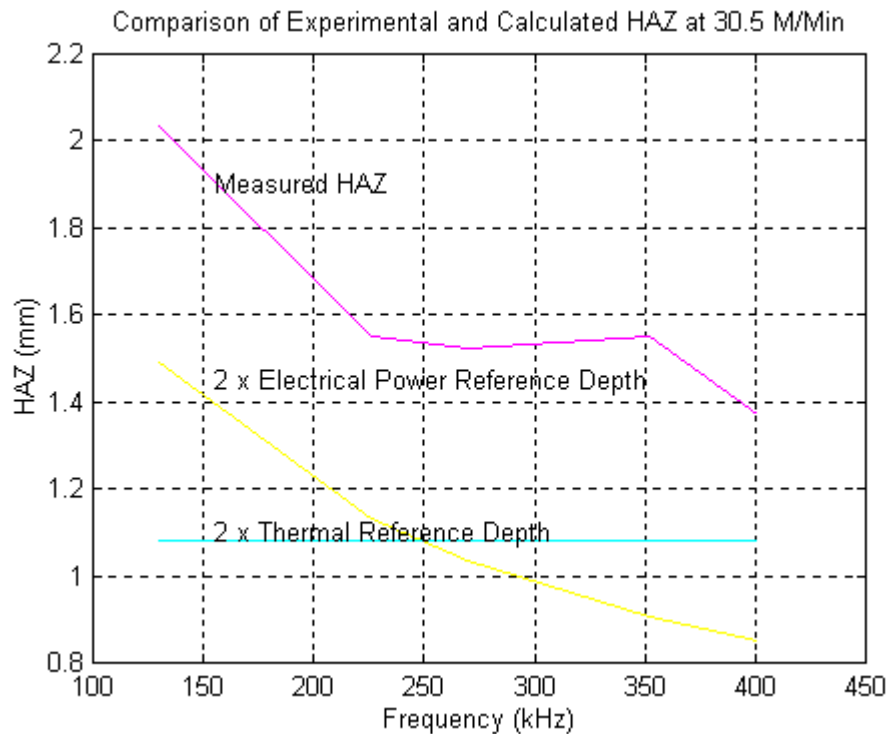


Figure 6 - Experimental and Calculated Heat Affected Zone at 30.5 M/Min

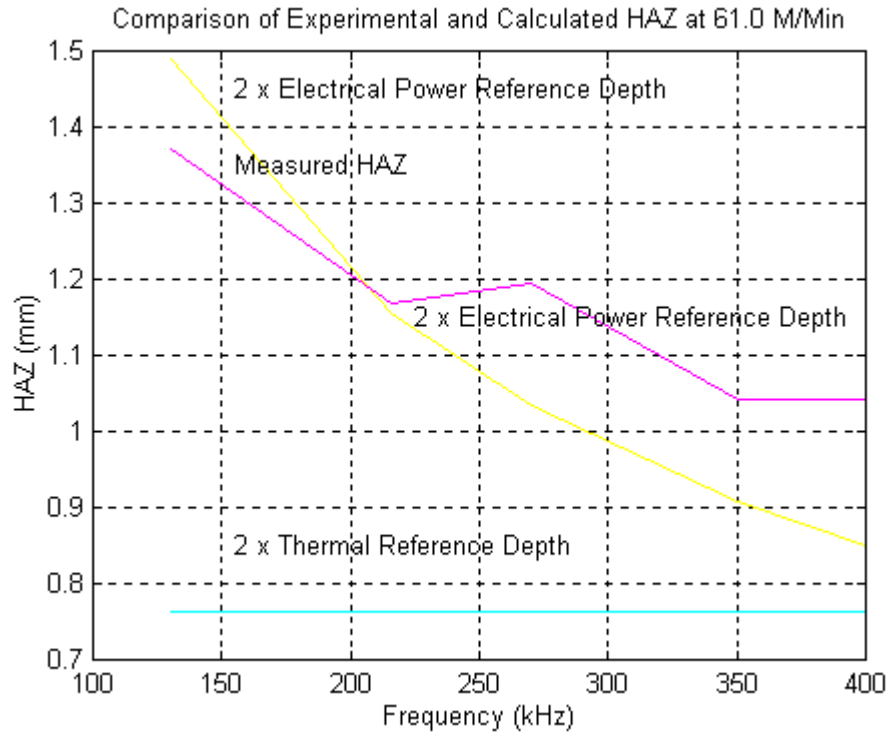


Figure 7 - Experimental and Calculated Heat Affected Zone at 61.0 M/Min

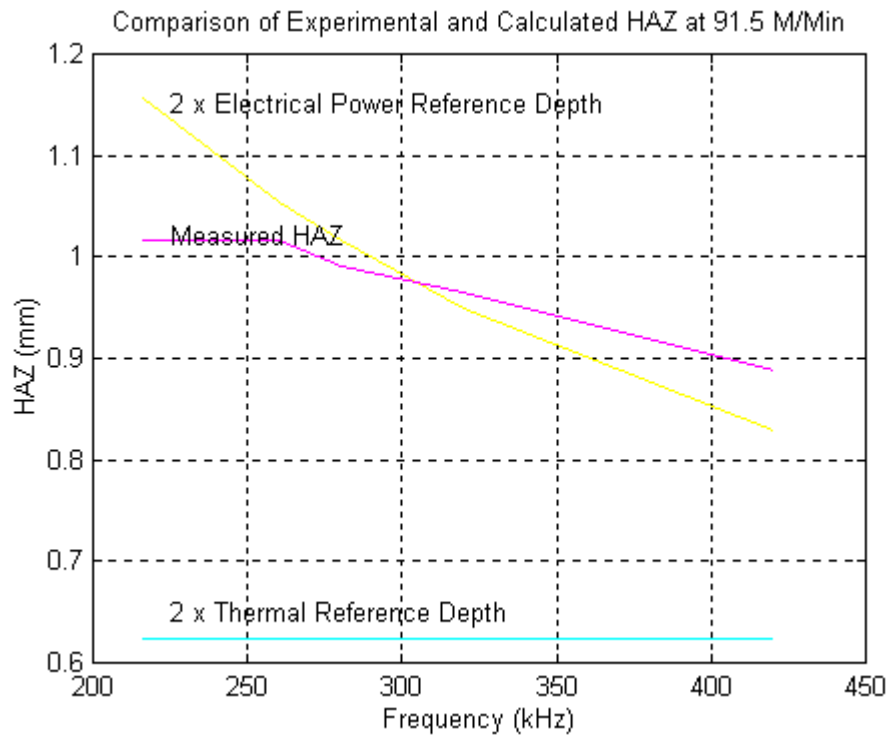


Figure 8 - Experimental and Calculated Heat Affected Zone at 91.5 M/Min

CONCLUSIONS:

The high frequency welding process has two distinct modes of operation that can be delineated by “Critical Mill Speed” or by “Critical Welding Frequency” for a particular tube geometry and material. When the welding process is operated substantially below the “Critical Mill Speed” or above the “Critical Welding Frequency”, the weld power requirement and the Heat Affected Zone in the “vee” is governed by the “thermal reference depth” and the process is said to be operating in the “Thermal Mode”. If the process is operated substantially above the “Critical Mill Speed” or equivalently, below the “Critical Welding Frequency”, the weld power and the size of the Heat Affected Zone in the “vee” is governed by the “electric power reference depth” and the process is said to be operating in the “Electric Power Mode”.

It is better to operate the process in the “Thermal Mode” than the “Electric Power Mode”. Operating in the “Thermal Mode” results in the lowest welding power requirement, the narrowest Heat Affected Zone, the lowest sensitivity to process parameter variations, and the lowest impeder magnetic flux level. This can be accomplished by selecting the welding frequency to be well above the “Critical Welding Frequency” for the highest expected mill speed.

APPENDIX I - Solution of Equation 7 to Obtain Equation 13

We wish to find a solution to:

$$K \frac{d^2 T(x, y)}{dx^2} - \rho C_p v_o \frac{dT(x, y)}{dy} + Q_o e^{-2x/\xi} \mu_{-1}(y) = 0 \quad (\text{A1})$$

with boundary conditions:

$$T(x, y = 0) = 0 \quad (\text{A2})$$

$$T(x = 0, y = y_o) = \Delta T \quad (\text{A3})$$

$$T(x \rightarrow \infty, y) = 0 \quad (\text{A4})$$

$$\left. \frac{dT(x, y)}{dx} \right|_{x=0} = 0 \quad (\text{A5})$$

First, take the Laplace Transform of Equation A1 with respect to y :

$$T(x, y) \Leftrightarrow \Theta(x, s) \quad (\text{A6})$$

so that:

$$\frac{d^2 \Theta(x, s)}{dx^2} - \frac{v_o s}{\varepsilon} \Theta(x, s) = -\frac{Q_o}{Ks} e^{-2x/\xi} \quad (\text{A7})$$

where:

$$\varepsilon \equiv \frac{K}{C_p \rho} \quad (\text{A8})$$

The resulting differential equation is linear and in the single variable, x . This is solved in the usual manner, finding both the homogeneous and particular solutions and applying boundary conditions A4 and A5. This yields:

$$\Theta(x, s) = \frac{Q_o \varepsilon e^{-2x/\xi}}{Kv_o s(s - \frac{4\varepsilon}{\xi^2 v_o})} - \frac{2Q_o \varepsilon^{3/2} e^{-\sqrt{v_o s/\varepsilon} x}}{\xi Kv_o^{3/2} s^{3/2} (s - \frac{4\varepsilon}{\xi^2 v_o})} \quad (\text{A9})$$

Since we want the temperature distribution at the “vee” edge, we evaluate A9 at $x = 0$ to get:

$$\Theta(x = 0, s) = \frac{Q_o \varepsilon}{Kv_o s(s - \frac{4\varepsilon}{\xi^2 v_o})} - \frac{2Q_o \varepsilon^{3/2}}{\xi Kv_o^{3/2} s^{3/2} (s - \frac{4\varepsilon}{\xi^2 v_o})} \quad (\text{A10})$$

We now invert the Laplace Transform using:

$$\frac{1}{s(s-a)} \Leftrightarrow \frac{1}{a}(e^{ay} - 1) \quad (\text{A11})$$

$$\frac{1}{\sqrt{s(s-a^2)}} \Leftrightarrow \frac{1}{a} e^{a^2 y} \text{erf}(a\sqrt{y}) \quad (\text{A12})$$

and

$$\frac{1}{s} F(s) \Leftrightarrow \int_0^y f(\eta) d\eta \quad (\text{A13})$$

so as to obtain:

$$T(y) = \frac{Q_o \xi^2}{4K} \left(e^{4\varepsilon y/\xi^2 v_o} - 1 \right) - \frac{2Q_o \varepsilon^{3/2}}{\xi Kv_o^{3/2}} \int_0^y \frac{\xi}{2} \sqrt{\frac{v_o}{\varepsilon}} e^{4\varepsilon \eta/\xi^2 v_o} \text{erf}\left(\sqrt{\frac{4\varepsilon \eta}{\xi^2 v_o}}\right) d\eta \quad (\text{A14})$$

The integral in Equation A14 has no closed form solution (at least known to this author!). However, a very tight mathematical bound exists for its kernelⁱⁱⁱ:

$$\frac{1}{x + \sqrt{x^2 + 2}} < e^{-x^2} \int_x^\infty e^{-t^2} dt \leq \frac{1}{x + \sqrt{x^2 + \frac{4}{\pi}}} \quad (\text{A15})$$

This can be used to show:

$$\int_0^y e^{ax} \text{erf}(\sqrt{ax}) dx = \frac{1}{a} \left[e^{ay} - 1 - \frac{4}{3\sqrt{\pi}\alpha} \left((ay + \alpha)^{3/2} - (ay)^{3/2} - \alpha^{3/2} \right) \right] \quad (\text{A16})$$

where:

$$\frac{4}{\pi} \leq \alpha < 2 \quad (\text{A17})$$

Finally, we get an expression for $T(y)$ which we evaluate at y_o and set equal to ΔT :

$$T(y = y_o) = \Delta T = \frac{Q_o \xi^2 \sqrt{\alpha}}{3\sqrt{\pi} K} \left[\left(\frac{4\varepsilon y_o}{\xi^2 v_o \alpha} + 1 \right)^{3/2} - \left(\frac{4\varepsilon y_o}{\xi^2 v_o \alpha} \right)^{3/2} - 1 \right] \quad (\text{A18})$$

We can now solve this equation for Q_o and use Equation 12 to obtain Equation 13.

APPENDIX II - Derivations of Equations 20, 22 & 23

For Equation 23 where $f_o \ll f_{critical}$ we assume that:

$$\frac{4y_o \varepsilon}{\xi^2 v_o \alpha} \ll 1 \quad (\text{B1})$$

so that:

$$\left[\left(\frac{4y_o \varepsilon}{\xi^2 v_o \alpha} + 1 \right)^{3/2} - \left(\frac{4y_o \varepsilon}{\xi^2 v_o \alpha} \right)^{3/2} - 1 \right] \cong \left[\left(\frac{4y_o \varepsilon}{\xi^2 v_o \alpha} + 1 \right)^{3/2} - 1 \right] \quad (\text{B2})$$

The term in parenthesis is now expanded in a binomial series and higher order terms are neglected:

$$\left(\frac{4y_o \varepsilon}{\xi^2 v_o \alpha} + 1 \right)^{3/2} \cong 1 + \left(\frac{3}{2} \right) \frac{4y_o \varepsilon}{\xi^2 v_o \alpha} \quad (\text{B3})$$

The bracketed term now becomes:

$$\left[\left(\frac{4y_o \varepsilon}{\xi^2 v_o \alpha} + 1 \right)^{3/2} - \left(\frac{4y_o \varepsilon}{\xi^2 v_o \alpha} \right)^{3/2} - 1 \right] \cong \frac{6y_o \varepsilon}{\xi^2 v_o \alpha} \quad (\text{B4})$$

Which when substituted into Equation 13 yields Equation 23. To obtain Equation 20, the bracketed term in the denominator of Equation 13 is rewritten as:

$$\left[\left(\frac{4y_o \varepsilon}{\xi^2 v_o \alpha} + 1 \right)^{3/2} - \left(\frac{4y_o \varepsilon}{\xi^2 v_o \alpha} \right)^{3/2} - 1 \right] = \left[\left(\frac{4y_o \varepsilon}{\xi^2 v_o \alpha} \right)^{3/2} \left[\left(1 + \frac{\xi^2 v_o \alpha}{4y_o \varepsilon} \right)^{3/2} - 1 - \left(\frac{\xi^2 v_o \alpha}{4y_o \varepsilon} \right)^{3/2} \right] \right]$$

It is now argued that for $f_o \gg f_{critical}$,

$$\left(\frac{\xi^2 v_o \alpha}{4y_o \varepsilon} \right) \ll 1 \quad (\text{B6})$$

and the same binomial expansion is used on the inner bracketed term of Equation B5. The result is substituted into Equation 13 to get Equation 20.

For Equation 22, we have the case where:

$$\left(\frac{\xi^2 v_o \alpha}{4 y_o \varepsilon} \right) = 1 \quad (\text{B6})$$

Substituting this into Equation 13 yields:

$$P_o = \frac{3\sqrt{\pi}\Delta T d y_o K}{2\xi\sqrt{\alpha}[\sqrt{2}-1]} \quad (\text{B7})$$

Now from Equation B6 we can also observe that:

$$1 = \frac{\xi}{2} \sqrt{\frac{v_o \alpha}{\varepsilon y_o}} = \frac{\xi}{2} \sqrt{\frac{C_p \rho v_o \alpha}{K y_o}} \quad (\text{B8})$$

Multiplying B7 and B8 gives Equation 22.

ⁱⁱ For a detailed discussion of “skin effect”, see for example: Ramo, S., Whinnery, J.R., and Van Duzer, T.; Fields and Waves in Communication Electronics; John Wiley & Sons; New York, New York, USA; 1984.

ⁱⁱ For example, see Oppenheimer, E.D.; Weld Heating Power Requirements form a Process Viewpoint; Tube Americas; Vol. V, No. 4; August 1994.

ⁱⁱⁱ Abramowitz, M. & Stegun, I.A.; Handbook of Mathematical Functions; Dover Publications; New York, New York; 1964; Result 7.1.13.